Energy Proceedings
Vol 59, 2025
ISSN 2004-2965

An isobaric compressed carbon dioxide system operating at high temperature#

Chuangang Bai[1], Xingpeng Yan[1], Kaiyue Zheng[1], Xiaohu Yang[2], Zhan Liu [1*]

1 College of Electromechanical Engineering, Qingdao University of Science and Technology, Qingdao 266061, PR China

2 School of Human Settlements and Civil Engineering, Xi'an Jiaotong University, Xi'an 710049, PR China
(Corresponding Author: zhanliu168@qust.edu.cn)

ABSTRACT

Compressed carbon dioxide energy storage has attracted considerable academic interest due to its benefits, including high efficiency and low investment costs. This paper investigates an isobaric carbon dioxide energy storage system and establishes a thermodynamic model to evaluate its system performance. The results indicate that higher pressure in the carbon dioxide high-pressure storage tank can increase the energy density of the system; however, it will reduce the system's round-trip efficiency. Increasing the reheater's preheating temperature during the energy storage process improves the system round-trip efficiency and energy density. At the same time, improving the reheater's split ratio, the low-pressure compressor's outlet pressure, and the cooling temperature of the first-stage cooler can improve the system round-trip efficiency and energy density.

Keywords: Energy storage, Compressed carbon dioxide, Isobaric system.

NONMENCLATURE

Abbreviations	
CAES	Compressed Air Energy Storage
CCES	Compressed Carbon dioxide Energy Storage
SC-CCES	Supercritical Carbon dioxide Energy Storage
Symbols	
$\dot{W}$	Power (W)
h	Specific enthalpy (J/kg)
$\dot{m}$	Mass flaw rate (kg/s)
$\dot{Q}$	Heat transfer rate (W)
t	Time (s)
RTE	Round-trip efficiency (%)

1. INTRODUCTION

To address energy depletion and optimize the energy structure, the scale of renewable energy development has been expanding significantly. However, renewable energy sources face challenges such as volatility and intermittency, which have led to growing academic interest in energy storage technologies. Compressed Air Energy Storage (CAES) presents a promising solution to the volatility and intermittency of renewable energy sources. However, traditional CAES systems are hindered by low energy density, primarily due to their excessively large storage volumes. Although liquefied air solutions can improve energy density, they present considerable technical challenges (air critical point: 3.77 MPa / -140.5°C) [1]. In contrast, CO_2 has a suitable critical point (7.38 MPa / 31.1°C), with significantly higher mass density and energy density compared to air, CO_2-based systems enable smaller equipment size and higher system energy density, which has attracted considerable interest from researchers. [2]

Zhang et al. [3] developed a compressed CO_2 energy storage (CCES) system, where CO_2 is stored in liquid and supercritical states within low-pressure and high-pressure tanks, respectively. This system utilizes a packed bed heat exchanger to store thermal and cold energy, enabling direct heat transfer and resulting in higher heat exchange efficiency. The round-trip efficiency (RTE) of the system is 60.69%, and the energy density is 8.07 kWh/m³. Additionally, the energy density of the CCES system is 2.8 times greater than that of the Advanced Adiabatic Compressed Air Energy Storage system.

He et al. [4] established a supercritical carbon dioxide energy storage system (SC-CCES), in which CO_2 is stored in a supercritical state within low-pressure and high-pressure tanks. The authors conducted both conventional and advanced exergy analyses for SC-CCES and CAES. The results revealed that the exergy efficiency

This is a paper for the 11th Applied Energy Symposium: Low Carbon Cities & Urban Energy Systems (CUE2025), July 18-22, 2024, Kitakyushu, Japan.

of SC-CCES is 57.02%, surpassing CAES (50.86%). Additionally, the RTE of SC-CCES reached 73.02%, significantly higher than CAES (60.65%).

Zhang et al. [5] addressed the issue of excessive storage volume of low-pressure CO2 by utilizing adsorbents to store low-pressure CO2 in an adsorption bed. This approach eliminates the need for CO2 liquefaction and reduces system complexity. Under the design conditions, the RTE and energy density of the system were 66.68% and 12.11 kWh/m3, respectively. Additionally, the storage density of low-pressure CO2 reached 390.94 kg/m3 at 298 K and 0.1 MPa.

The systems described in References 3-5 utilize constant-volume storage tanks. A critical issue arises during operation: as the system operates, the pressure within the tank fluctuates, causing the compressor to operate under off-design conditions. This deviation results in reduced the system's efficiency.

Isobaric systems provide a valuable alternative to constant-volume systems by maintaining stable tank pressure through pressure compensation. Pottie et al. [6] conducted a comparison between constant-volume and isobaric systems. When the effects of compressor deviations from design performance were disregarded, the constant-volume system achieved a RTE of 57.8%, which is lower than the 61.5% RTE of the isobaric system. When compressor deviations were taken into account, the RTE of the constant-volume system was approximately 10% lower than that of the isobaric system. Consequently, the isobaric system holds significant research value.

Zhang et al. [7] developed a novel energy storage system that combines CCES with CAES. This system integrates a low-pressure CO_2 storage chamber into the high-pressure air storage chamber of the CAES system. The low-pressure CO_2 chamber utilizes a flexible gas bladder, whose volume adjustments enable isobaric operation of the CAES system. Experimental results indicate that at a charging/discharging pressure of 5.5 MPa, the system achieves an efficiency of 67.47%, representing a 12% improvement compared to conventional CAES systems that operate under a charge pressure of 10 MPa and a discharge pressure of 3.5 MPa.

Liu et al. [8] coupled isobaric CAES with wind power generation and investigated the accommodation capacity of unstable wind power by simulating underwater static pressure to achieve isobaric operation. The research has found that, despite the constantly changing load, the use of Proportional-Integral-Derivative controller to regulate the speed of the piston compressor can achieve a stable (less than 1.5% fluctuation) discharge pressure of the compressor, completely absorbing unstable wind power generation.

In summary, utilizing CO_2 as the working medium and adopting an isobaric system offer numerous advantages. This paper integrates the benefits of both CO_2-based systems and isobaric systems, proposing a novel design in which CO_2 and water are co-stored in a high-pressure tank. Isobaric operation is achieved by regulating the inflow and outflow of water.

2. SYSTEM DESCRIPTION

The schematic diagram of the system is shown in Fig. 1. At the start of the energy storage, low-pressure CO_2 is stored in a gas chamber which is made of flexible materials in a gaseous state, and high-pressure CO_2 is stored in a liquid state in high-pressure storage tank (HPST), the flexible Gas Chamber for low-pressure gaseous CO_2 is filled with CO_2 at ambient temperature and pressure. The HPST is filled with high-pressure water. Low-pressure CO_2 is extracted from the gas chamber, preheated by Reheater#1 (RH1), and compressed by Low-Pressure Compressor (LPC) and High-Pressure Compressor (HPC). The compression heat generated during this process is stored in two thermal storage units (HT1, LT1 and HT2, LT2), The operating temperature of this system is relatively high, so the first two sets of thermal storage use molten salt as the medium, each utilizing different molten salts: SolarSalt for the first unit and HitecXl for the second. The high-pressure CO_2 is then split in Cooler#3 (IC3). One stream returns to RH1 to reheat the inlet of the LPC, while the other continues cooling in IC3, with its heat stored in a third thermal storage unit (HT3, LT3) that uses water as the medium. The two CO_2 streams from RH1 and IC3 are combined, cooled to ambient temperature in Radiator, and stored in the HPST. Simultaneously, water in the HPST is discharged, passes through a water turbine (WT) to produce electricity, and is stored in a water storage tank (WST) to maintain isobaric storage of high-pressure CO_2.

At the start of the energy release, a water pump (WP) pressurizes water from the WST to match the HPST pressure and injects it into the HPST, displacing liquid CO_2 at a constant pressure. The discharged liquid CO_2 splits into two streams: one enters Heater#1 (IH1), and the other flows through Reheater#2 (RH2) to recover waste heat from the Low-Pressure Turbine (LPT). After mixing the two streams, they continue to absorb heat from the third thermal storage unit (HT3, LT3) in IH1, and expand through High-Pressure Turbine (HPT) and LPT to produce electricity. Finally, the CO2 is cooled in RH2 and returned to the low-pressure carbon dioxide gas chamber.

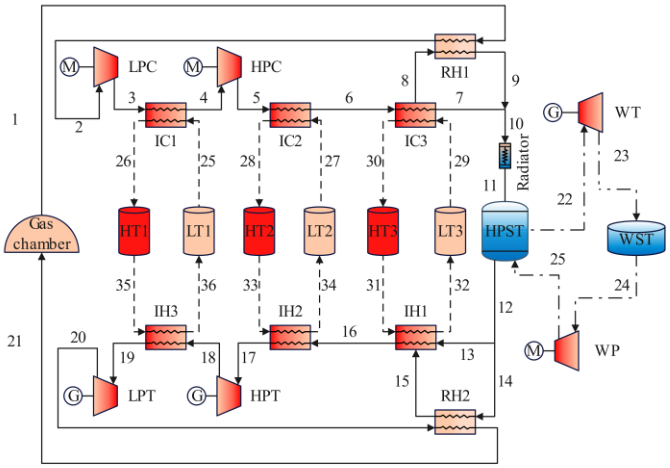

Fig. 1 Schematic diagram of the proposed system

3. MATHEMATIC MODEL

In order to explore the performance of the system, the thermodynamic model of the system is established. The model is based on the law of conservation of mass and the law of conservation of energy.

The power consumed by compressors is:

$$\dot{W}_{LPC} = \frac{\dot{m}_2(h_3 - h_2)}{\eta_{Motor}\eta_{Gear}} \quad (1)$$

$$\dot{W}_{HPC} = \frac{\dot{m}_4(h_5 - h_4)}{\eta_{Motor}\eta_{Gear}} \quad (2)$$

in which $\dot{W}$ is the power scale and $\dot{m}$ is the mass flow rate. η_{Motor} is the motor efficiency; η_{Gear} is the gear efficiency; *h* stands for the fluid's specific enthalpy.

The output power process of expanders is as follows:

$$\dot{W}_{HPT} = \dot{m}_{17}(h_{17} - h_{18})\eta_{Motor}\eta_{Gear} \quad (3)$$

$$\dot{W}_{LPT} = \dot{m}_{19}(h_{19} - h_{20})\eta_{Motor}\eta_{Gear} \quad (4)$$

The thermodynamic process of heat exchangers is as follows:

$$\dot{Q} = \dot{m}_{hot}(h_{in} - h_{out})_{hot} = \dot{m}_{cold}(h_{out} - h_{in})_{cold} \quad (5)$$

where $\dot{Q}$ is the heat transfer rate.

The output power of water turbine is:

$$\dot{W}_{WT} = \dot{m}_{22}(h_{22} - h_{23})\eta_{Motor}\eta_{Gear} \quad (6)$$

The output power of water pump is:

$$\dot{W}_{WP} = \frac{\dot{m}_{24}(h_{25} - h_{24})}{\eta_{Motor}\eta_{Gear}} \quad (7)$$

The power consumed during the charging process is:

$$\dot{W}_{in} = \dot{W}_{LPC} + \dot{W}_{HPC} - \dot{W}_{WT} \quad (8)$$

The output power during the discharging process is:

$$\dot{W}_{out} = \dot{W}_{HPT} + \dot{W}_{LPT} - \dot{W}_{WP} \quad (9)$$

Round-trip efficiency (*RTE*) is defined as the ratio of net work output to net work input:

$$RTE = \frac{\dot{W}_{out} t_{dis}}{\dot{W}_{in} t_{ch}} \times 100\% \quad (10)$$

in which t_{dis} is the discharge time; t_{ch} is the discharge time.

Energy density is defined as the ratio of the output power to the volume of the HPST:

$$\rho_E = \frac{\dot{W}_{out} t_{dis}}{V_{HPST}} \quad (11)$$

in which the V_{HPST} is the volume of the HPST.

4. RESULTS AND DISCUSSION

This section analyzes the impact of key parameters on the system performance. The basic design parameters of the system are summarized in Table 1.

Table 1

Main baseline parameters of the system

Parameter	Unit	Value
Ambient pressure	MPa	0.1
Ambient temperature	K	293.15
Polytropic efficiency	%	90
Motor and Generator	%	98.5
Gear efficiency	%	99
Output power	MW	100
Charge time	h	8
Discharge time	h	8

4.1 Effect of HPST pressure

Fig. 2 shows the variations in system RTE and energy density with changes in the pressure of the HPST. As shown, both parameters exhibit monotonic trends: when the pressure increases from 10 MPa to 16 MPa, the system RTE decreases from 75.96% to 75.41%, while the energy density increases from 102 kWh/m³ to 120.7 kWh/m³.

Fig. 3 shows the variation in the system's powers as the pressure of the high-pressure tank changes. When the pressure increases from 10 MPa to 16 MPa: The power of the LPC monotonically decreases from 118.53 MW to 107.88 MW; the power of the HPC monotonically increases from 12.15 MW to 24.58 MW; The power of the Water Turbine (WT) rises from 2.43 MW to 3.30 MW; The power of the HPT decreases from 96.53 MW to 87.87 MW; The power of the LPT increases from 9.17 MW to 18.96 MW; The power of the WP increases from 3.00 MW to 4.08 MW. Meanwhile, the and remain nearly constant at 128.72 MW and 102.73 MW, respectively.

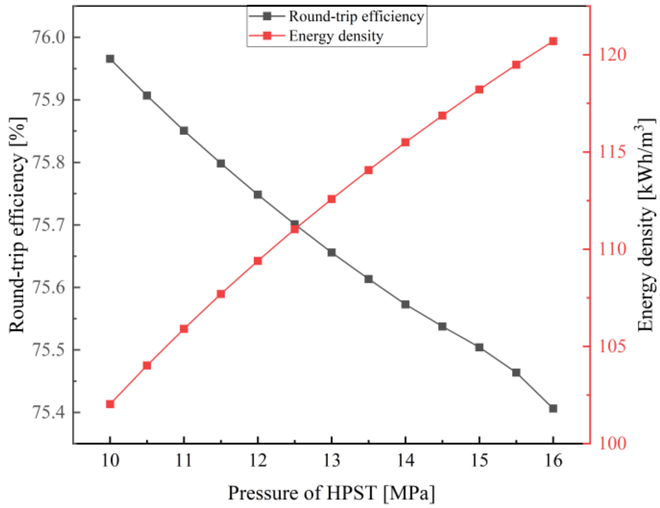

Fig. 2 Impact of the HPST Pressure on the system round-trip efficiency and energy density

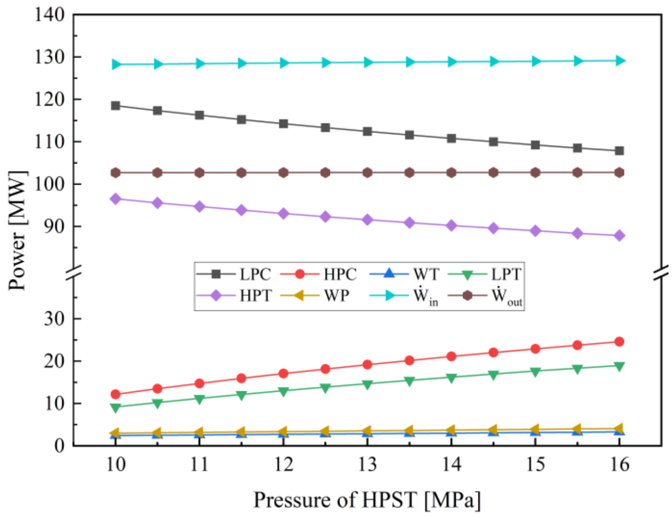

Fig. 3 Impact of the HPST Pressure on the system powers

4.2 Effect of RH1 preheating temperature

Fig. 4 shows the impact of changes in the RH1 preheating temperature (temperature of state 8) on the system RTE and energy density. As the preheating temperature increases from 70°C to 118°C, both the system RTE and energy density exhibit monotonically increasing trends. The system RTE rises from 75.39% to 75.71%; the energy density increases from 109.1 kWh/m³ to 119.9 kWh/m³.

Fig. 5 shows the impact of changes in the RH1 preheating temperature on the system powers. As the preheating temperature increases from 70°C to 118°C, the power of each fluid machine remains largely unchanged: the power of the LPC remains at 110.68 MW, the HPC remains at 21.25 MW, the WT remains at 3.03 MW, the HPT remains at 90.14 MW, the LPT remains at 16.34 MW, and the WP remains at 3.75 MW. Meanwhile, the and stay nearly constant at 128.89 MW and 102.74 MW, respectively.

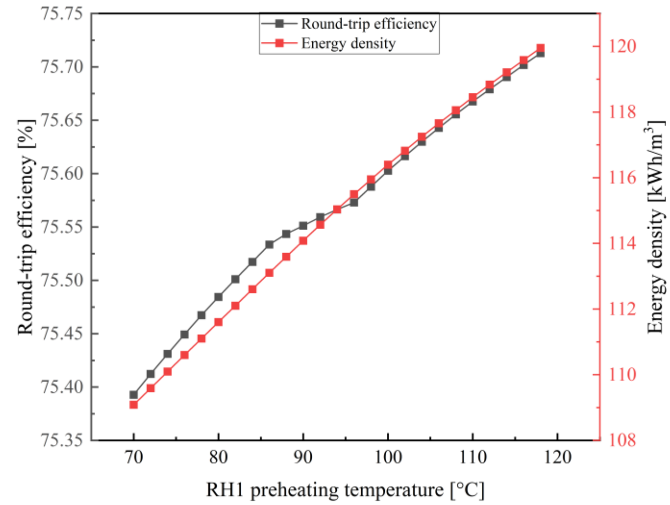

Fig. 4 Impact of RH1 preheating temperature on the system round-trip efficiency and energy density

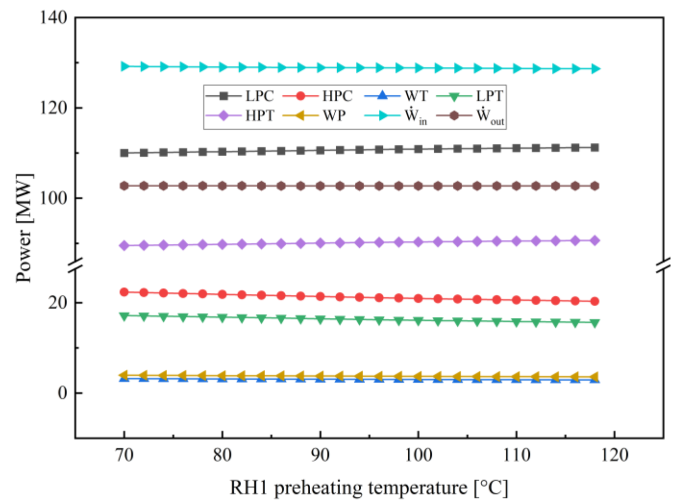

Fig. 5 Impact of RH1 preheating temperature on system powers

4.3 Effect of the reheater split ratio

Fig. 6 shows the impact of the reheater split ratio on the system RTE. From the graph, it can be seen that the higher the split ratio of the two reheaters, the higher the system efficiency. The maximum system efficiency of 75.62% occurs when the split ratio of stream 8 to stream 6 is 0.5 and the split ratio of stream 14 to stream 12 is 0.4.

Fig. 7 shows the impact of the reheater split ratio on the system energy density. As shown, when the split ratio of the stream 8 to stream 6 configuration is fixed, the system energy density remains nearly unchanged as the split ratio of stream 14 to stream 12 changes. In contrast, the split ratio of the stream 8 to stream 6 configuration significantly influences the system energy density. When the stream 14 to stream 12 split ratio is held constant, increasing the stream 8 to stream 6 split ratio results in a rising trend in system energy density. The maximum energy density of 115.6 kWh/m³ is achieved at a higher split ratio of the stream 8 to stream 6 configuration.

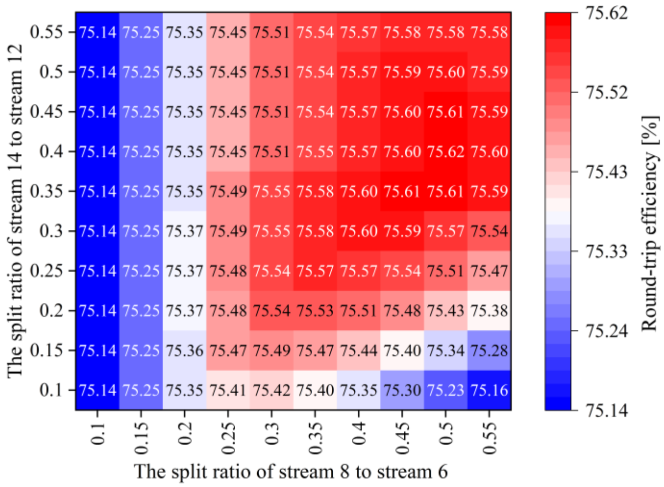

Fig. 6 Impact of split ratio of two reheaters on system round-trip efficiency

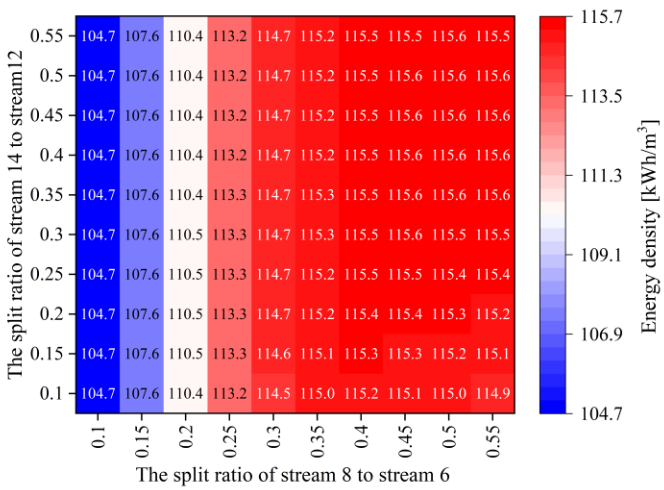

Fig. 7 Impact of split ratio of two reheaters on system energy density

4.4 Effect of outlet pressure of the LPC and the IC1 cooling temperature

Fig. 8 shows the impact of outlet pressure of the LPC (pressure of state 3) and the IC1 cooling temperature (temperature of state 25) on the system RTE. It can be observed that when the outlet pressure of LPC is fixed, the system RTE increases as the IC1 cooling temperature rises from 270 °C to 310 °C. Similarly, when the IC1 cooling temperature is fixed, the system RTE also increases as the outlet pressure of LPC increases from 4.6 MPa to 7 MPa. Therefore, the maximum system efficiency of 75.63% occurs at the maximum values of both parameters: the IC1 cooling temperature and the outlet pressure of LPC.

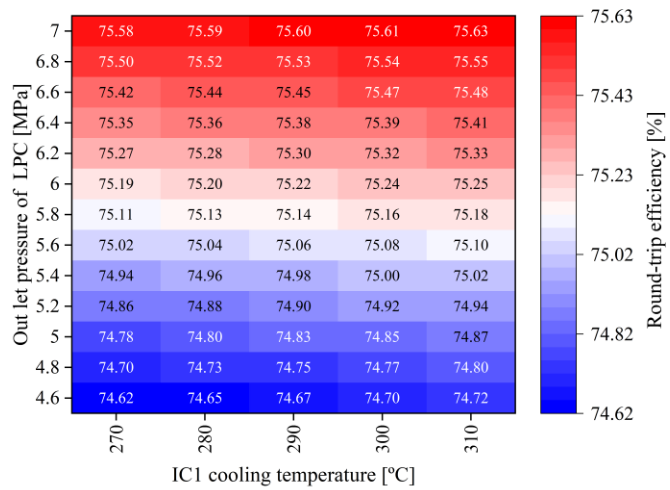

Fig. 8 Impact of LPC outlet pressure and the IC1 cooling temperature on system round-trip efficiency

Fig. 9 shows the impact of IC1 cooling temperature and LPC outlet pressure on the system energy density. As the IC1 cooling temperature increases from 270°C to 310°C, the energy density shows an overall upward trend. Moreover, at the same temperature, as the outlet pressure increases, the energy density also increases. Therefore, the maximum system energy density occurs at the highest values of both the LPC outlet pressure and IC1 cooling temperature, reaching 117.2 kWh/m3.

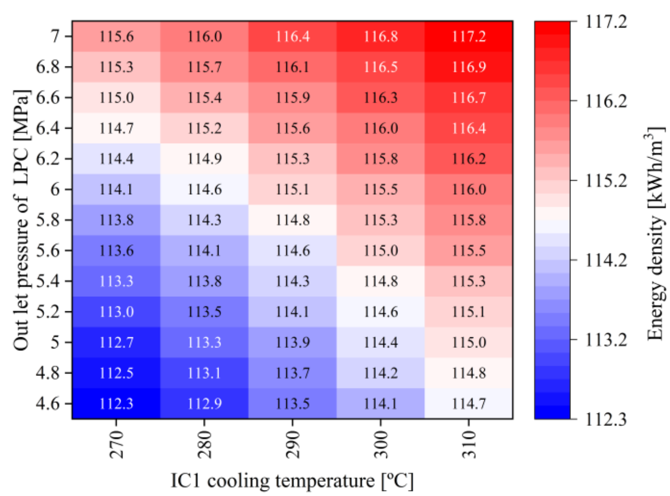

Fig. 9 Impact of outlet pressure of LPC and the IC1 cooling temperature on system energy density

5. CONCLUSIONS

This paper establishes and investigates the performance of an isobaric carbon dioxide system. The main conclusions are as follows: As the storage pressure of the high-pressure tank increases, the system round-trip efficiency and energy density exhibit opposing trends—energy density increases while round-trip efficiency decreases. Increasing the preheating temperature of the reheater in the energy storage process improves the system's round-trip efficiency and energy density. Increasing the split ratios of both reheaters improves the system round-trip efficiency and energy density. Additionally, raising the outlet pressure of the low-pressure compressor and the cooling temperature of the first-stage cooler can also improve the system round-trip efficiency and energy density. The pressure of the carbon dioxide high-pressure tank and the reheater's preheating temperature during energy storage have minimal impact on the power consumption of the energy storage process and the power output of the energy release process.

ACKNOWLEDGEMENT

NONE

REFERENCE

[1] Nabat MH, Zeynalian M, Razmi AR, et al. Energy, exergy, and economic analyses of an innovative energy storage system; liquid air energy storage (LAES) combined with high-temperature thermal energy storage (HTES). Energ Convers Manage 2020;226:113486.

[2] Li Y, Yu H, Tang D, et al. A comparison of compressed carbon dioxide energy storage and compressed air energy storage in aquifers using numerical methods. Renew Energ 2022;187:1130-1153.

[3] Zhang Y, Yang K, Hong H, et al. Thermodynamic analysis of a novel energy storage system with carbon dioxide as working fluid. Renew Energ 2016; 99: 682–697.

[4] He Q, Liu H, Hao Y, et al. Thermodynamic analysis of a novel supercritical compressed carbon dioxide energy storage system through advanced exergy analysis. Renew Energ 2018;127:835-849.

[5] Zhang T, Gao J, Zhang Y, et al. Thermodynamic analysis of a novel adsorption-type trans-critical compressed carbon dioxide energy storage system. Energ Convers Manage 2022;270:116268.

[6] Pottie D, Cardenas B, Garvey S, et al. Comparative Analysis of Isochoric and Isobaric Adiabatic Compressed Air Energy Storage. Energies 2023;16(6):2646.

[7] Zhang Y, Liu J, Yin S, et al. Design and performance analysis of a novel compressed air–liquid CO2 energy storage. Energ Convers Manage 2024; 301: 118068.

[8] Liu C, Su X, Yin Z, et al. Experimental study on the feasibility of isobaric compressed air energy storage as wind power side energy storage. Appl Energ 2024; 364: 123129.